



Rainstorm and flooding characteristics and simulated analysis in the Loess Plateau, China

Tong Nie¹ · Lichan Li² · Xiaohui Jiang¹ · Yuxin Lei¹ · Chun Deng¹ · Wenjuan Cai¹ · Jiaying He¹

Received: 26 July 2023 / Accepted: 1 March 2024 / Published online: 3 April 2024
© The Author(s), under exclusive licence to Springer Nature B.V. 2024

Abstract

In recent years, human activities have caused significant changes in the underlying surface and affected the processes of rainstorms and floods. It is of great practical significance for water resources management to understand the mechanism of the rainstorm and flood process under the changing conditions of land use and cover change (LUCC) and grasp the change law of the rainstorm and flood. Given this, this study aims to take the flood simulation of the Kuye River basin in the Loess Plateau as an example, selecting the measured flood data for the last 60 years (1960–2018) for statistical analysis and then illustrating the effect of the LUCC on the storm flooding using the distributed time varying gain hydrological model (DTVGM). The primary outcomes are as follows: (1) The statistical results show that the four rainstorm indicators of the annual maximum one-hour precipitation, the annual maximum precipitation, the number of days with ≥ 25 mm precipitation, and the number of days with ≥ 50 mm precipitation have no apparent increasing trend during the study period. (2) During the study period, the most significant annual flood peak discharge and the frequency of heavy and moderate floods in the basin decreased significantly ($p < 0.01$). (3) By constructing the DTVGM model, it was found that the flood flow showed a significant reduction during the simulation period, with an attenuation rate of about 40%, subject to changes in the underlying surface conditions. Discussing the impacts of changes in the LUCC on the Kuye River basin flood processes will enable better formulation of water resources management policies. This integrated research methodology is expected to serve as a reference for other river basins and help build a more sustainable water resource management system for rational utilization and adequate protection of water resources.

Keywords The kuye river basin · Storm flood characteristics · LUCC · Distributed time varying gain model (DTVGM)

✉ Xiaohui Jiang
xhjiang@nwu.edu.cn

¹ College of Urban and Environmental Science, Northwest University, Xi'an 710127, PR China

² CNACG Underground Space Technology Co.,Ltd, Xi'an 710127, PR China

1 Introduction

Global flooding will increase due to human-induced climate and land surface changes (Hirabayashi et al. 2013; Hirsch and Archfield 2015; Zhang et al. 2015; Zuo et al. 2023). Flood-related disasters threaten human production and life (Kia et al. 2012; Zhu et al. 2017). Human activities have had a significant impact on the environment, constantly altering the natural environment, leading to changes in the underlying surface conditions of the watershed, affecting the hydrological cycle process, and influencing the regional flooding process to some degree (Li et al. 2015; Lv et al. 2023). Changes in the underlying surface caused by human activities add uncertainty to future flood predictions. It is imperative to determine changes in flood features and their responses to changes in land use and cover change (LUCC) to expose the impact of human activities on future rainstorms and flood processes.

Changes in the underlying surface resulting from human activities, such as the deployment of water conservation and soil conservation measures, changes in land use, and increases in vegetation coverage (Liu et al. 2014a; Wang et al. 2007a, 2010), are crucial to reducing soil erosion, flood peaks, and flood catastrophes. Large-scale soil and water conservation initiatives have considerably affected the underlying surface conditions, further influencing the hydrological regime of the region. Since the implementation of the “converting farmland to forest and grassland” policy in 1999, runoff and sediment in most areas of the Yellow River Basin have shown a significant downward trend (Hu et al. 2011a; Zhao et al. 2016); however, the distribution of precipitation in the middle reaches of the year is uneven, and the rainfall time is short, the rainfall intensity is high. Rainstorms are frequent (Zhang et al. 2020). In addition to climate factors, the majority of scholars believe that soil and water conservation measures, such as terraced fields and water retention, and human activities, such as water abstraction, are the primary factors contributing to runoff reduction (Gu et al. 2018, 2021; Li et al. 2021), which has a significant impact on flood reduction. Changes in land use are the most direct manifestation of the influence of human activities on the subsurface. Land use changes will alter the near-surface cover’s water-intercepting capacity, impacting the regional distribution of precipitation. This will directly impact the water production capacity of the surface, which will affect the hydrological cycle in the watershed and the flood characteristics (Abbo et al. 2003; Erena and Worku 2019; Zare et al. 2016). Szwagrzyk et al. (2018) predicted that, depending on the scenario, the peak flow of the Ropa River would either decline owing to forest expansion or remain unchanged, indicating that land use change has a minimal effect on the hydrology of mountain watersheds. Pal et al. (2022) thought that under the influence of future climate and land changes, the increase in precipitation and the conversion of natural vegetation to agricultural land and construction land would expand the area impacted by severe flooding. Gao et al. (2016) utilized the topography-based Hydrological Model (TOPMODEL) to simulate. They discovered that changes in plant cover on mild slopes are more likely to induce changes in flood levels than in vegetation cover on steep slopes. The initial investigations demonstrate that the alteration of the underlying surface significantly impacts the flood situation. Identifying the driving mechanism of the underlying surface change in rainstorms and floods has practical implications for the basin’s water resources planning, management, and development.

Rainstorms are one of the primary elements influencing flooding in the basin; therefore, a quantitative examination of their relationship with flooding has significant scientific importance for water resource management. According to existing research, the cumulative

rainfall in 7 days and the maximum rainfall in 3 and 12 h can be used as indications of a rainstorm since the incidence of floods is mainly related to the rise or severity of precipitation (Ren et al. 2022). Relevant studies have shown that rainstorms considerably affect flood volume and peak flow (Sheng et al. 2022). Currently, the majority of studies on the law of rainstorms and floods use hydrological data recorded in the basin to investigate the evolution of rainstorms, rainstorms, and floods and their internal relationship (Wang et al. 2019, 2021). Under the effect of a rainstorm, however, there is little research on the influence of the LUCC on the flooding process and limited quantitative research results (Fu et al. 2020; Yao et al. 2016). The influence mechanism of LUCC on flooding is frequent under the conditions of discrete rainstorms. Therefore, we aim to reveal the mechanisms by which changes in the LUCC affect the occurrence and development of floods under heavy rainfall conditions and to provide a more scientific basis for water resource management.

Few studies have studied the causes of the drop in the Kuye River basin's flood peak discharge and its reaction to changes in the LUCC (Ma et al. 2021; Wang et al. 2013). However, the Kuye River basin is a typical Loess Plateau region. The watershed is extensively eroded, there are regular natural disasters, and the ecological ecosystem is fragile (Liang et al. 2013). Changes in hydrological characteristics in this region have direct ties to the prevention and control of flood disasters, the allocation of water resources, and the ecological protection of water in the entire Yellow River basin. Observational data indicate precipitation has not reduced much in recent years; however, the annual runoff and flood peak flow have declined. The Distributed Time Varying Gain Hydrologic Model (DTVGM) is widely used in runoff simulation (Xia et al. 2023; Yang et al. 2023; Yu et al. 2023), and it can simulate the spatial and temporal distribution of hydrologic processes in a watershed. Consequently, this paper aims to examine the changes in rainstorms and floods in the Kuye River basin over the past 60 years and determine the characteristics of long-term changes in rainstorms and floods at the regional scale. Using DTVGM, examine the effect of LUCC on the law of storms and floods.

The primary aims of this paper are as follows: (1) analyze the long-sequence variation characteristics of precipitation and flood in the Kuye River basin (2) Using the DTVGM model to simulate flood changes (3) The parameters before and after the land use change are used to simulate the flood to quantitatively evaluate the impact of the LUCC on the flooding process. The parameters before and after the LUCC are used to simulate the flood to quantitatively evaluate the impact of the land use change on the flooding process. This study will improve the ecological environment of the Kuye River and even the entire Loess Plateau, reduce soil erosion, and improve water quality.

2 Data and methods

2.1 Study area

The Kuye River basin is located on the right bank of the main channel of the Yellow River in China, runs from the northwest to the southeast, and eventually joins the Yellow River in Shenmu County. The topography is mountainous in the northwest and low in the southeast, and the river is 221 km long (Fig. 1). The watershed stretches from 38°N to 40°N and 109°E to 111°E, having an area of 8706km². The Kuye River is a rainstorm area with

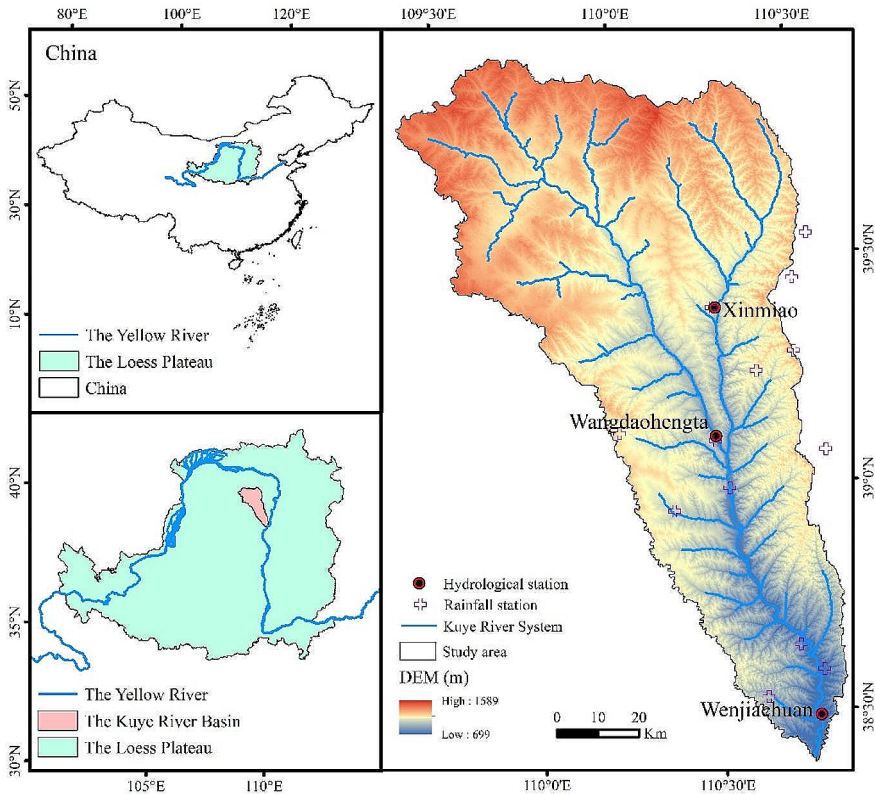


Fig. 1 Geographical location of kuye river basin

frequent floods and is one of the primary sources of floods in the north mainstream of the Yellow River. The annual mean precipitation is 419 mm, while the annual mean temperature is 7.9 °C. Cultivated land is primarily dispersed in the lower terrain sections in the center and southeast. In contrast, forest land and grassland are primarily distributed in the higher terrain areas in the southeast and northwest. There are primary hydrological stations in the Kuye River basin, such as Xinmiao, Wangdaohengta, and Wenjiachuan, among which Wenjiachuan Hydrological Station is the basin's control station.

2.2 Data

Xinmiao Station, Wangdaohengta Station, and Wenjiachuan Station of the watershed control station provided most of the data used in this study. The “Yellow River Basin Hydrological Yearbook” provides precipitation and flood data from 1960 to 2018 for three hydrological stations in the basin. In addition, 14 rainfall stations in the Kuye River basin were chosen to collect precipitation data from 1960 to 2018. A basin hydrological model requires geographical, meteorological, and hydrological data and socioeconomic information. Geospatial data include the Digital Elevation Model (DEM), LAI datasets, land use, and soil types. Meteorological and hydrological data include precipitation data collected by rainfall stations,

evapotranspiration data collected by meteorological stations and hydrological databases, and socioeconomic data comprised of population and GDP. See Table 1 for information.

2.3 Methods

2.3.1 Mutation test

1. Sliding t-test: Mutations are tested by examining whether the difference between the mean values of two subsequences in an element sequence is significant (Du et al. 2019). If the difference between the two subsequences exceeds the significance level, it is considered a mutation.
2. Mann-Kendall mutation test: is a commonly used nonparametric test (Mann 1945). For a sequence X with a sample size of n , at a given significance level α , if $|UF_k| > UF_{\alpha}$, it shows that there is a clear trend change in the series. Inverse sequence value $UB_k = -UF_k$, the intersection of curves and between the critical lines is the abrupt point.

2.3.2 DTVGM model

DTVGM is founded on a combination of distributed hydrological simulation and hydrological nonlinear system technique (Hou et al. 2018). The model has been utilized frequently at the watershed scale and is appropriate for runoff simulations in the Northwest of China (Xia et al. 2004, 2018; Yang et al. 2022) but rarely for flood simulations. Based on the traditional TVGM model, the DTVGM model pulls the feature data of the underlying surface using remote sensing technologies and a GIS platform. The initially established unit TVGM is refined into the basin unit by dividing it by the DEM based on the basin slope aspect. Then,

Table 1 Data information

Datasets	Resolution	Sequentially	Source
Precipitation data	/	1960–2018	Yellow River Basin Hydrological Yearbook, China Meteorological Data Network(https://data.cma.cn/)
Flood data	/	1960–2018	Yellow River Basin Hydrological Yearbook
Evapotranspiration data	/	1960–2018	China Meteorological Data Network(https://data.cma.cn/)
DEM	90 m*90m	/	Resource and Environment Science and Data Center(www.resdc.cn)
Land use Data	1 km*1km	1980, 1990, 2000, 2015	
LAI	8 km*8km	1982–2018	
Soil type dataset	1 km*1km	2000	
Population Density Data	1 km*1km	2000	
Socioeconomic Data	1 km*1km	2000	

runoff and confluence calculations are performed for watersheds. The study area is located in arid and semiarid regions; rainfall runoff is dominated by hyperosmotic runoff, and there is a nonlinear relationship between rainfall and runoff. In order to capture its nonlinear nature from system theory, the flood of the Kuye River basin was calibrated and verified based on the characteristics of the basin’s underlying surface, the time varying gain hydrological nonlinear system model, and the flood data.

The water balance formula of DTVGM can be as follows(Mao et al. 2016):

$$P_i + AW_i = AW_{i+1} + g_1 \left(\frac{AW_{ui}}{WM_u C_j} \right)^{g_2} P_i + AW_{ui} K_r + Ep_i \left(\frac{AW_{ui}}{WM_u C_j} \right) + AW_{gi} K_g \quad (1)$$

P is precipitation (mm); AW is soil moisture (mm); AW_u is upper soil moisture; AW_g is lower soil moisture; WM_u is upper saturated soil moisture; g₁ and g₂ are parameters of time-varying gain factor (0 < g₁ < 1, g₂ > 1); C is land cover parameter; Kr is soil water outflow coefficient (0 < K_r < 1); Kg is groundwater runoff coefficient (0 < K_g < 1); Ep_i is the potential evapotranspiration; i is the time period; and j is the number of sub-basins. by calculating soil water runoff and calculating subsurface water runoff using. Equation g₁(AW_{ui}/WM_uC_j)^{g₂}P_i is used to calculate surface runoff, by AW_{ui}K_r calculating soil water runoff and calculating subsurface water runoff using AW_{gi}K_g.

The DTVGM model can simulate and reflect the heterogeneity of numerous hydrological elements and surface variables. Using GISNET to evaluate the slope, aspect, flow direction, current accumulation matrix, terrain index, and sub-basins extraction of the original DEM data, the Kuye River basin was divided into 39 sub-basins. There are numerous model parameters (Table 2), but the following parameters are determined and calibrated based on the application experience of the model: the flow production calculation parameters g₁ and g₂, the infiltration rate fc from the upper layer to the lower layer, the soil water outflow coefficient kr, and the groundwater outflow coefficient krg. In this article, the Nash efficiency coefficient (NSE) and the coefficient of determination (R²) are utilized as model evaluation criteria (Nash and Sutcliffe 1970; Gupta et al. 1999).

The flowchart of the methodology of this paper is shown in Fig. 2.

Table 2 Selected parameters of the DTVGM model

Parameters	Parameter Meaning	Parameter value range	Final value range
g ₁	Production flow calculation parameter	0–1	0.01–0.02
g ₂	Production flow calculation parameter	1–5	0.25–0.26
k _r	Soil water outflow coefficient	0–1	0.01–0.02
krg	Groundwater outflow coefficient	0–1	0.1–0.2
f _c	The permeability coefficient from the upper layer to the lower layer	0-1000	0.01-4
RoughRss	Manning formula roughness factor	0.001-10	0.7-1
Wmi	Minimum water content of soil water	0–1	0.8-1

3 Results

3.1 Rainstorm variation characteristics

According to the number of rainstorms, grades, and intensity, we select four indicators for statistical analysis: annual maximum one-hour precipitation, annual maximum precipitation, days of ≥ 25 mm precipitation, and days of ≥ 50 mm precipitation for statistical analysis (Fig. 3). Each indicator shows a negligible upward trend and a moderate growth rate from 1960 to 2018. The maximum value of annual precipitation, the annual maximum precipitation, and the number of days with precipitation ≥ 25 mm all happened after 2000, while the minimum value occurred before 2000. Statistics indicate that precipitation increased after 2000 compared to the 1980 and 1990 s. The intensity and frequency of precipitation in the 1980 and 1990 s were the lowest in the long-term record.

3.2 Flood variation characteristics

3.2.1 Maximum flood peak discharge characteristics

As shown by the annual flood peak flow of the enormous flood at the Wenjiachuan Hydrological Station, the control station in the research region (Fig. 4), the flood peak flow of the most significant flood in the Wenjiachuan Basin declined dramatically between 1960 and 2018 ($p < 0.01$). The flood peak in the 1960 and 1970 s has an average value of $5297 \text{ m}^3/\text{s}$,

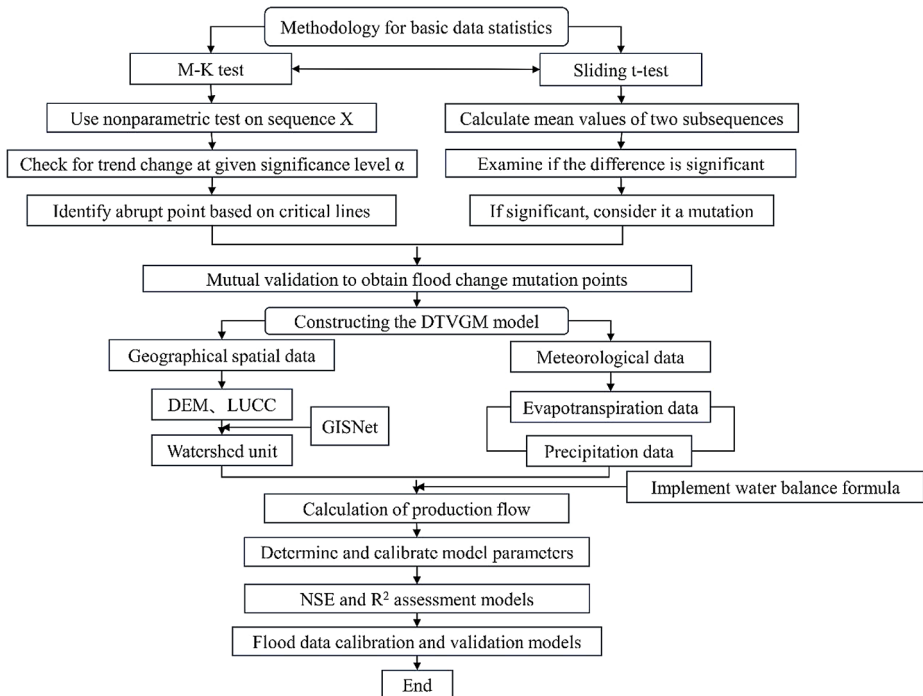


Fig. 2 Methodology flowchart

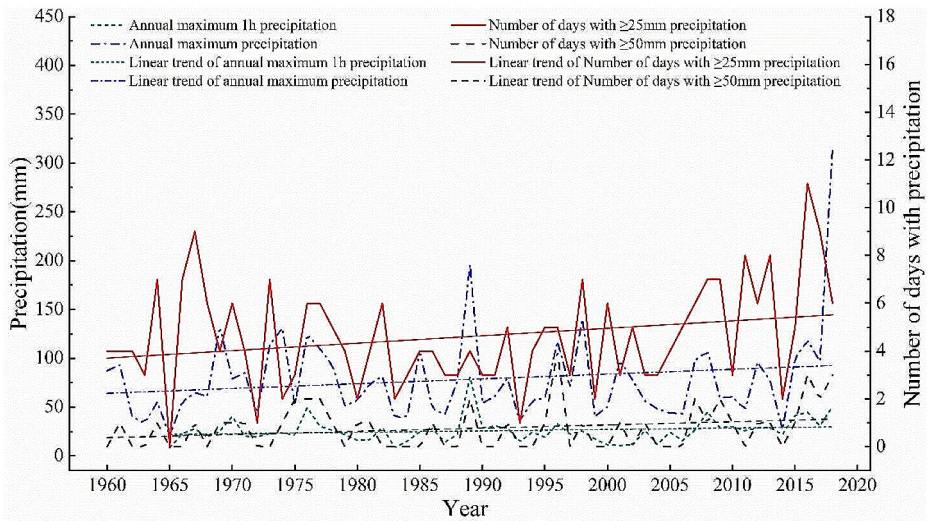


Fig. 3 Characteristics of annual rainstorm indicators

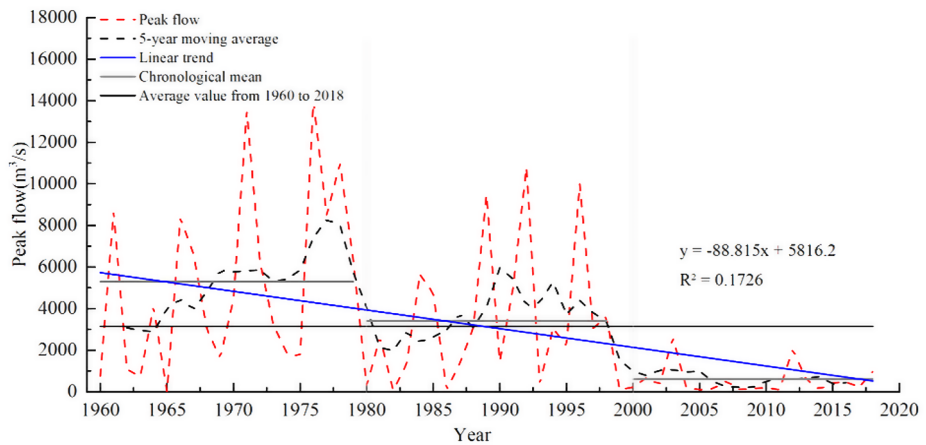


Fig. 4 Maximum annual flood peak discharge of Wenjiachuan station

the highest value in the entire sequence. The three floods in 1971, 1976, and 1978 had a flow rate of more than 10,000 m³/s. The peak flood flow declined in the 1980 and 1990 s, averaging 3419 m³/s. From 2000 to 2018, the flood peak flow averaged only 610 m³/s, representing only 19.3% of the multi-year average.

3.2.2 Changes in frequency of large and moderate floods

After calculating the average flood peak value of the enormous flood at Wenjiachuan station over the years, which was 3151m³/s, the study used 1/2 and 1/4 of this average value as the standard for large-scale and medium-scale floods, sorting and plotting the change process

of the occurrence times of large-scale and medium-scale floods separately (Fig. 5). During the 1960 and 1970 s, the average yearly frequency of floods exceeding moderate levels in the Kuye River watershed was 2.2 times. During the 1980 and 1990 s, there were 1.30 times as many moderate floods. After 2000, the number of occurrences declined drastically, with none occurring more than once. In the 1960 and 1970 s, the average annual frequency of large-scale flooding increased by 1.5 times. In the 1980 and 1990 s, the frequency of large-scale floods was 1.1 times. After the year 2000, the frequency drops below one. After the 1980 and 1990 s, the frequency of large and medium floods in the Kuye River basin declined dramatically, and there were no large flood discharges after 2000.

3.2.3 Flood peak variability analysis

Calculate the flood peak sequence data UF (red) and UB (blue) for the Wenjiachuan hydrological station and construct the curve. If a point of intersection between curves UF and UB is within the critical line ± 1.96 , this point is regarded as the time node of the sequence mutation. Through the M-K test (Fig. 6a), we found that the intersection point of the two curves of UF and UB was in 1998. We initially thought that the mutation point of the flood sequence was in 1998, which, combined with the results of the analysis of the sliding T-test method, as shown in Fig. 6b, confirms that the annual maximum flood flow of Wenjiachuan Station was mutated in 1998.

In combination with the actual survey data, there has been neither a significant change nor an increase in rainstorms, although there is a definite downward trend in the peak flow. In the 1960s, many water retention and conservation measures were established in the Kuye River. The circumstances of the underlying surface continue to change, and the flood peak continues to diminish. After 1997, extensive coal mining operations were conducted in the Kuye River basin, drastically altering the underlying surface of the watershed. The mutation

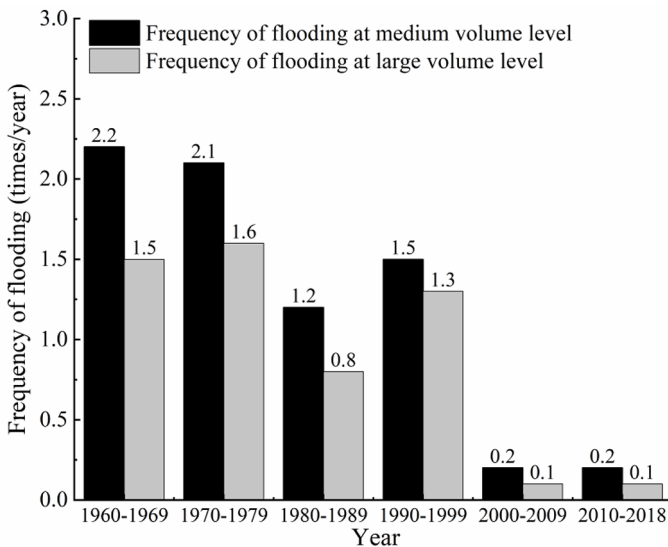


Fig. 5 Changes in the frequency of flooding at large and medium volume level

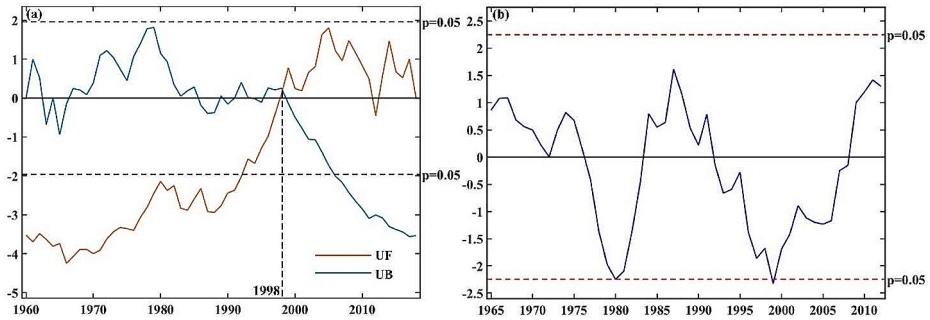


Fig. 6 Mutation point test of flood peak variation at Wenjiachuan station: (a) M-K test (b) Sliding t-test

years produced using statistical methods align with the actual scenario; hence, the mutation point data can be utilized in future research.

3.3 Flood simulation results

3.3.1 Analysis of simulation results of flood base period

According to the previous article, the sequence of annual maximum flood peak discharge in the Kuye River basin changed drastically in 1998. Before the abrupt change in the Kuye River basin, 11 flood data from 1966 to 1997 were utilized to develop the model. Six can be calibrated model parameters, while the remaining five were used to check model parameters. The outcomes are displayed in Table 3; Fig. 7. The correlation coefficients are all above 0.8 except for 1989; the NSE of the calibration period is more significant than 0.65, and in the verification period, is greater than 0.61; the R^2 is more significant than 0.6 in the simulation period. Moreover, the flood peak errors are within 10%, and the most simulated outcomes exceed the actual values. In conclusion, the DTVGM model developed using the rainstorm flood data may be applied to modeling the base period flood process.

3.3.2 Analysis of simulation results in flood change period

Table 4; Fig. 8 demonstrate that the simulation results are significant. The inaccuracies of the computed flood peaks for the eight simulated floods are all within 10%. The NSE for the calibration period is all larger than 0.60, while the simulation findings for the entire verification period are more accurate, with NSE greater than 0.65 and R^2 over 0.70. It can be observed from Tables 3 and 4, and Figs. 6 and 7 that throughout the simulation of the flooding process in the study region by the DTVGM model, the flood peak flow error of each flood is relatively minor. In other words, the simulation flood peak effect is improved, but the flood volume still deviates during the simulation. The model simulates single-peak floods more effectively than multiple-peak floods.

Table 3 Flood simulation of the base period in the Kuye River basin

Simulation period	Flooding field	Actual measured flood flow (m ³ /s)	Simulated flood flow (m ³ /s)	Error (%)	Correlation coefficient	NSE	R ²
Calibration period	19,670,728	5671	5776	-1.85	0.885	0.740	0.783
	19,680,725	1703	1666	2.17	0.873	0.678	0.762
	19,760,801	13,707	13,253	3.31	0.781	0.668	0.610
	19,770,727	7034	7005	0.4	0.916	0.818	0.839
	19,780,829	8963	8104	9.58	0.876	0.764	0.767
	19,790,807	6300	6490	3.01	0.848	0.670	0.618
Validation period	19,810,724	1805	1730	4.16	0.878	0.764	0.770
	19,840,727	4562	4216	7.58	0.842	0.657	0.708
	19,850,805	4435	4227	4.69	0.831	0.642	0.603
	19,880,804	3079	2877	6.56	0.845	0.636	0.713
	19,890,719	8694	8096	6.87	0.703	0.616	0.645

3.4 The impact of land use change on floods

3.4.1 Analysis of the effect of LUCC on flooding

The previous two sections demonstrate that the DTVGM model applies to the Kuye River Basin and can be used to examine the effect of changes in the watershed's underlying surface on flood characteristics. Therefore, the sorted rainstorm data of 15 fields may be inputted into the models based on these two sets of parameters, such that the precipitation factor can be considered unchanged and the difference generated from the simulation results from the change in land use. The flood peak flow after the alteration of the LUCC is reduced compared to before the change, as shown in Table 5, and the flood peak attenuation rate exhibits a changing 40% downward trend. As depicted in Fig. 9, the flood peak flow after the change is less than the flood peak flow before the change, indicating that the modification of the land use change of the watershed reduces the flood peak flow, and human activities have lowered the flooding process in the watershed. In addition, based on the flood simulation effect depicted in the figure, the shape of a giant flood stays consistent before and after the change, indicating that human activities primarily reduce the peak flow of the flood and alter its magnitude without affecting its duration. For minor flood processes, the change is not only reflected in the peak flow but also in a short delay in the duration of the flood.

Comparing the flood simulation before and after the land use change reveals that many model parameters have altered. These parameters primarily reflect changes to the surface beneath. In other words, the production flow calculation parameter falls, but both the soil water outflow coefficient and permeability coefficient from the upper to lower layer increase. Increased infiltration of the upper layer into the lower layer is closely associated with vegetation growth and coal mining. The decrease in flood peak results from increased water storage capacity and infiltration capacity of the underlying surface, caused by increased vegetation and conversion of cultivated land to grassland and forest land.

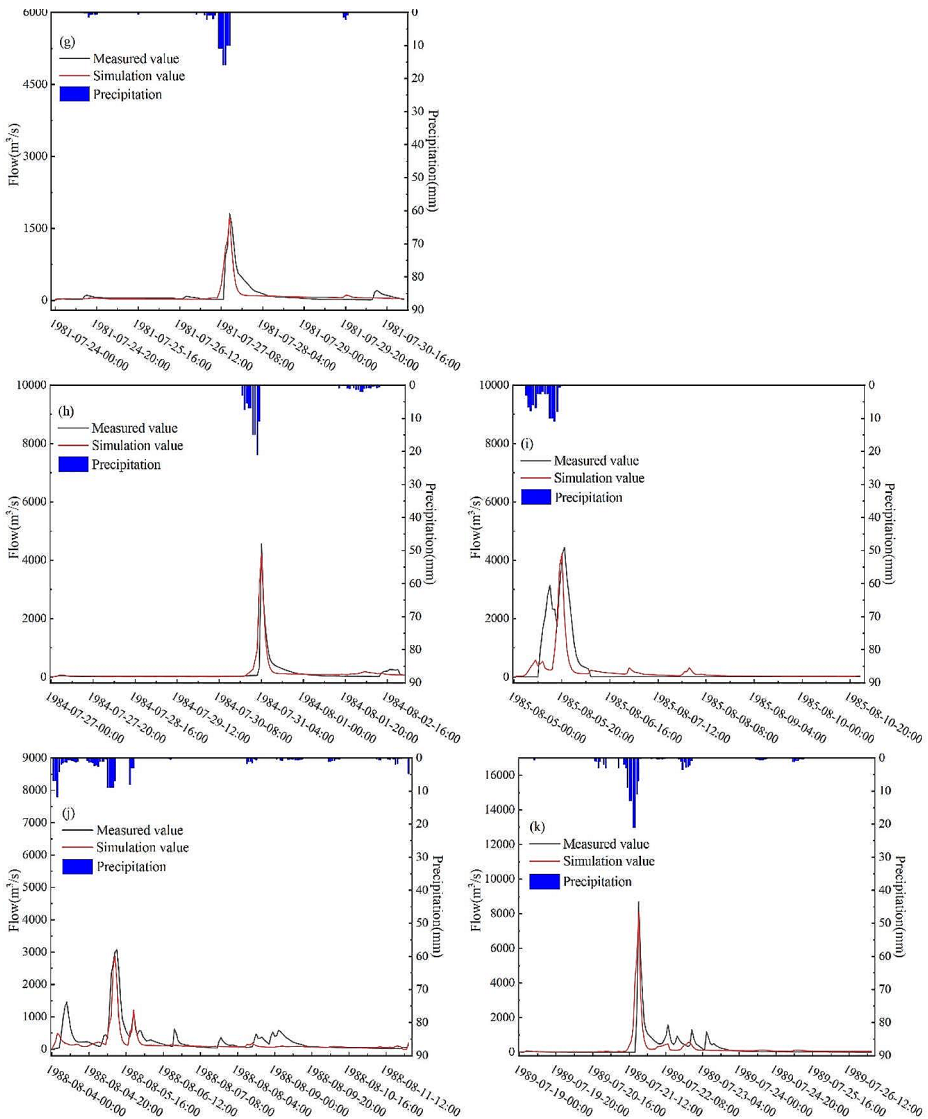


Fig. 7 Flooding process simulation in base period: (a) 1967; (b) 1968; (c) 1976; (d) 1977; (e) 1978; (f) 1979; (g) 1981; (h) 1984; (i) 1985; (j) 1988; (k) 1989

3.4.2 Influence of changes in the LUCC on the relationship between precipitation and flooding

Figure 10 depicts the link between precipitation and flooding. The flood peak flow after the mutation point is smaller in the same precipitation scenario. In the study of Sect. 3.1, the precipitation in the 1980 and 1990 s was less than in the 1960 and 1970 s. Consequently, the peak flow in this stage was much lower than in the 1960 and 1970 s due to precipitation. After 2000, precipitation increased gradually, but its peak flow reduced dramatically.

Table 4 Flood simulation in the changing period of the Kuye River basin

Changing period	Flooding field	Actual measured flood flow (m ³ /s)	Simulated flood flow (m ³ /s)	Error (%)	Correlation coefficient	NSE	R ²
Calibration period	20,060,809	115	122	-6.09	0.718	0.638	0.844
	20,070,827	515	557	-8.16	0.746	0.639	0.809
	20,100,811	177	193	-9.04	0.722	0.802	0.682
	20,120,720	2050	2154	-5.07	0.861	0.692	0.742
	20,130,729	569	606	-6.50	0.850	0.638	0.803
Validation period	20,150,801	453	444	1.99	0.813	0.717	0.834
	20,160,815	452	456	-0.89	0.871	0.665	0.759
	20,180,806	954	963	-0.94	0.847	0.668	0.718

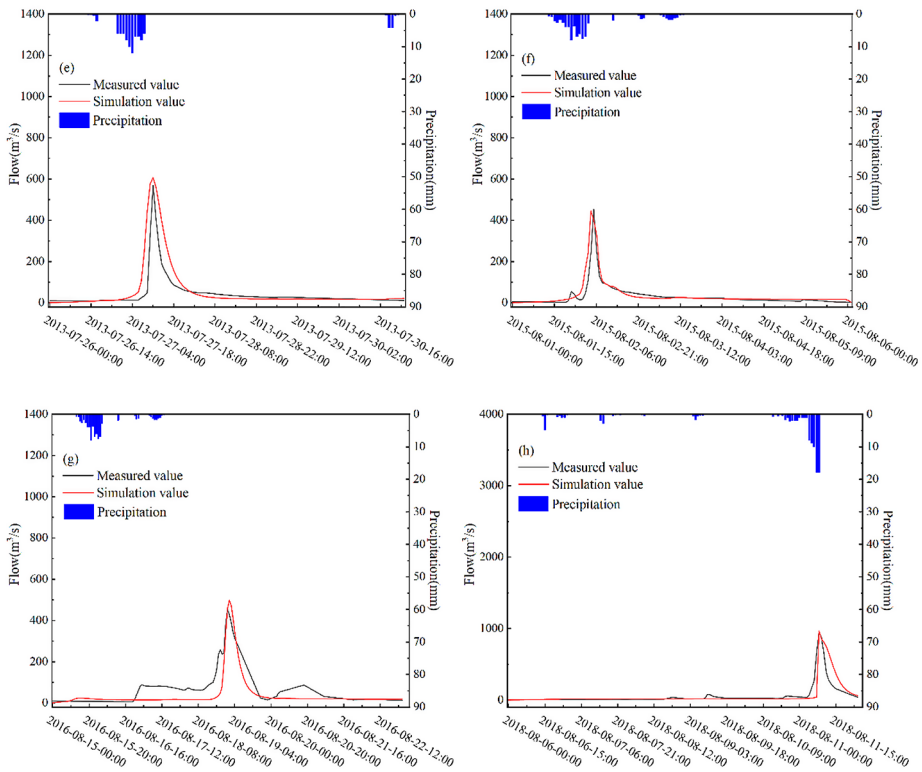


Fig. 8 Flood process simulation in change periods: (a) 2006; (b) 2007; (c) 2010; (d) 2012; (e) 2013; (f) 2015; (g) 2016; (h) 2018

This change was primarily the result of human activity. The purpose of establishing a linear relationship between precipitation and flooding is to qualitatively demonstrate the effect of land use changes on it. As illustrated in Fig. 10, the connection between precipitation and flood peak flow altered substantially in 1998. Figure 11(a) shows the spatial changes in land use in the study area from 1980 to 2015, with the most significant change in the area of coal land. The change in land use caused the change in flood peaks. Consistent with the conclu-

Table 5 Influence of LUCC on flood simulation results of the Kuye River basin

Flooding field	Flood peak flow before change (m ³ /s)	Flood peak flow after change(m ³ /s)	Flood peak attenuation rate(%)
19,670,728	5776	4568	20.9
19,680,725	1666	1092	34.5
19,760,801	13,253	8883	33.0
19,780,829	8104	4679	42.3
19,810,724	1730	743	57.1
19,840,727	4216	2294	45.6
19,850,805	4227	2574	39.1
19,890,719	8096	6371	21.3
20,060,809	336	115	65.7
20,070,827	951	557	41.1
20,120,720	2589	2154	16.8
20,130,729	1485	606	59.1
20,150,801	992	444	55.2
20,160,815	819	456	44.3
20,180,806	1712	963	43.8

sions from the DTVGM model simulations in this chapter, anthropogenic modifications to the underlying surface have drastically lowered the flood peak flow.

4 Discussion

Changes in underlying surfaces as a result of human activities, such as changes in land use, the implementation of water conservation measures, and increases in vegetation cover (Liu et al. 2014b; Wang et al. 2007b, 2010), are crucial to reducing soil erosion, flood peaks, and flood disasters. Since 1999, a series of environmental protection initiatives have greatly improved the vegetation in the basin(Liu et al. 2014c). The runoff and sediment in most areas of the Loess Plateau show a significant downward trend (Hu et al. 2011b; Zhao et al. 2016). Implementing water conservation measures such as check dams and reservoirs has altered the nature of the underlying surface of the watershed (Guo et al. 2019). In addition, many coal mining watersheds impact the underlying surface, resulting in changes in the interaction between rainfall and runoff (Luan et al. 2020; Jiang et al. 2010; Liu et al. 2022). These activities have contributed directly or indirectly to the reduction of peak flows.

4.1 Influence of vegetation restoration on flood

The model simulations show that anthropogenic impacts on flooding have significantly reduced peak flood flows before and after the land use change. The LAI data input by the model indicates that the vegetation conditions of the Kuye River basin have greatly improved (Fig. 12), demonstrating that the ecological measures implemented in China have shown astounding results (Zhao et al. 2013). Since the 1990s, the area covered by trees has expanded dramatically, and vegetation restoration measures have resulted in significant greening of the study area (Table 6). According to extant research figures, the greening trend of the Loess Plateau is evident, particularly after adopting the policy of returning cropland

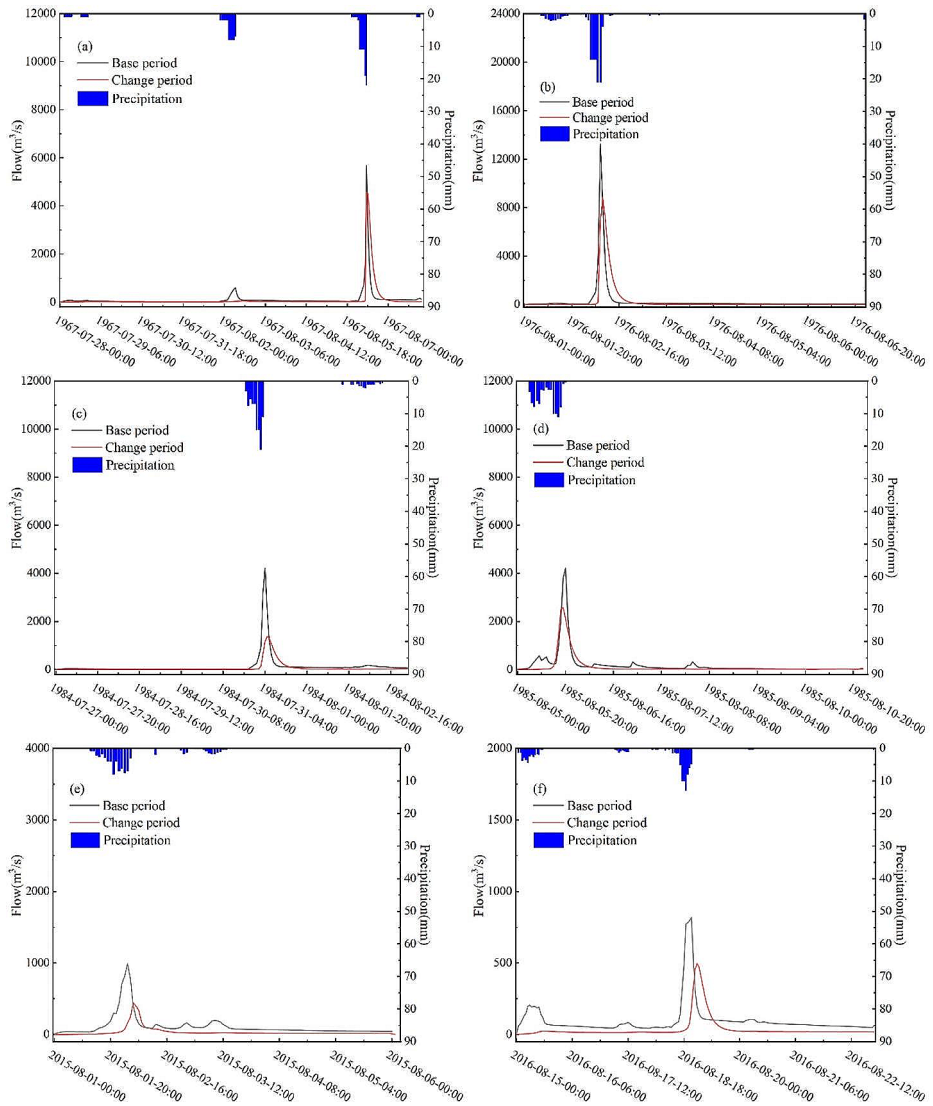


Fig. 9 Simulation of flood process before and after the change of land use change: (a) 1967; (b) 1976; (c) 1984; (d) 1985; (e) 2015; (f) 2018

to forests and grassland (Piao et al. 2015). Increased vegetation cover will influence the development of runoff. Through plant leaves, stems, and litter, the kinetic energy of rainfall is reduced, the amount of rainfall infiltration is increased, and surface runoff and its velocity (Fu et al. 2017). The annual growth rate of vegetation coverage in the Kuye River basin has increased dramatically since 2000. The visible improvement of vegetation will increase the amount of precipitation absorption and surface water consumption. The conversion of cultivated land to grassland and forest land, on the other hand, would result in changes to soil qualities, which will enhance the infiltration of watersheds. Moreover, vegetation will

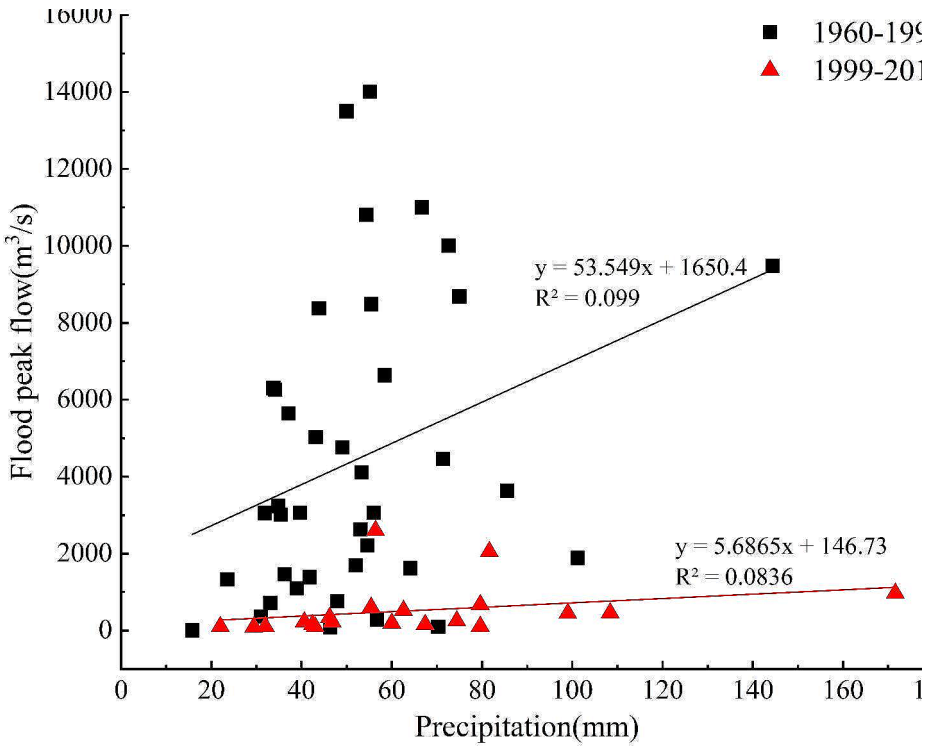


Fig. 10 Relation between precipitation and flood peak in different years in the kuye river basin

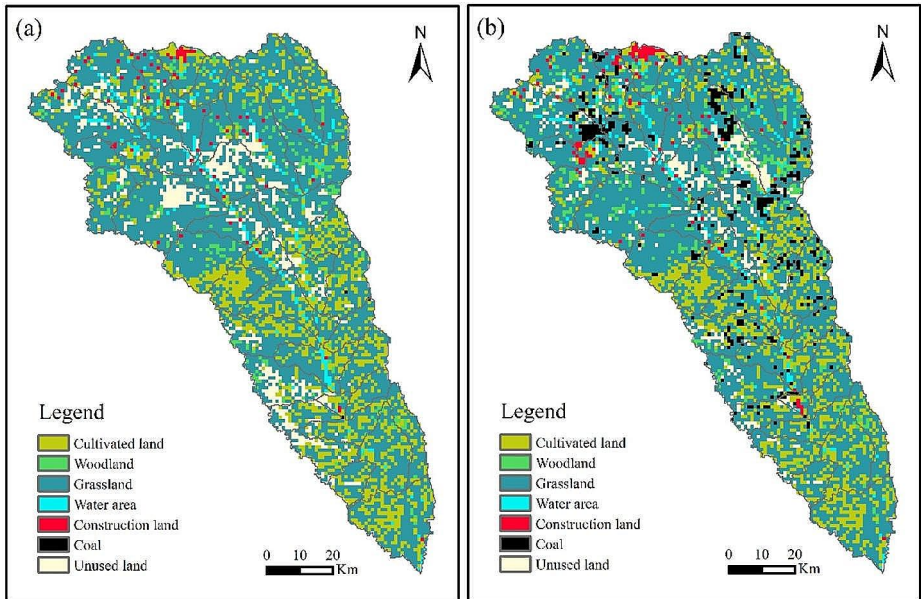


Fig. 11 Spatial distribution of land use in the Kuye River basin (a): 1980; (b): 2015

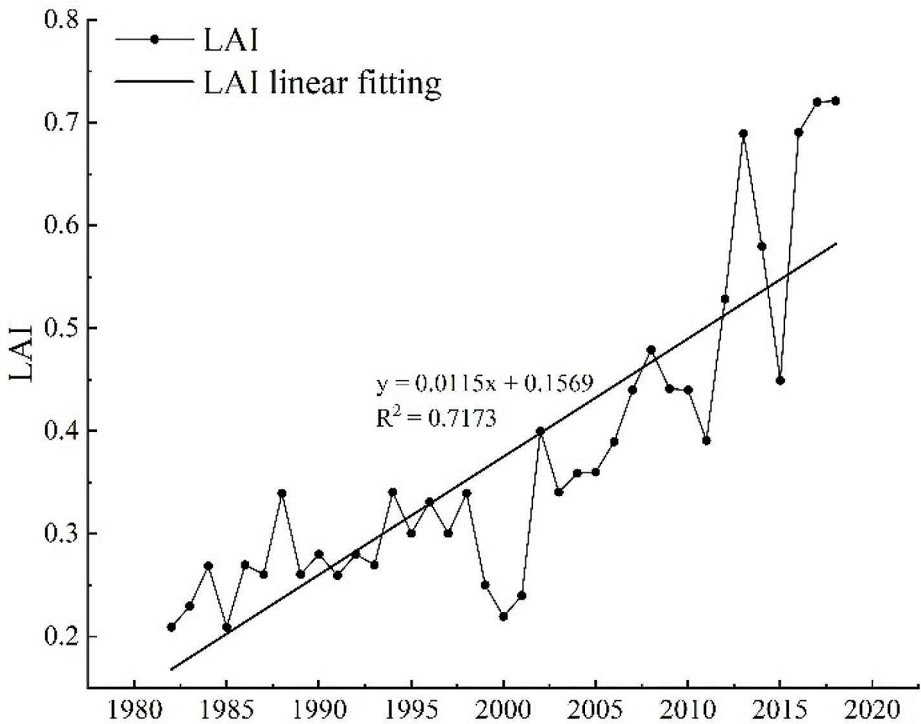


Fig. 12 Changes in leaf area index in the kuye river basin

extend the runoff confluence process and increase runoff infiltration, affecting the flood development in the basin.

4.2 Influence of land use on flood

In combination with the land use data input into the model, it is discovered that the area utilized for coal has changed dramatically and impacted the simulated watershed's flooding process. The area of coal land changed significantly from 1980 to 2015 (Fig. 13). Figure 13(a) shows the area percentage of land use in the study area, showing that forest land and coal land are the most significant changes. Figure 13(b) shows the increasing area percentage of forest and coal land under the flood reduction trend. Around 1998, large-scale coal mining was carried out in the Shenmu mining area in the basin, and the proportion of coal mining areas increased significantly from 1980 to 2015. Most coal mines in the Kuye River basin are in hilly regions with rugged terrain, deep valleys, and a few rivers, predominantly seasonal rivers. In the coal mining process, roadways and gobs form after mining is completed. After the area is gradually expanded, surface subsidence will be formed. Subsequently, the movement of the upper rock layer, deformation, and destruction will occur and even develop to the surface, causing large-scale surface subsidence (Qu et al. 2020). These will significantly impact the natural state of surface water and groundwater and destroy the underground impermeable layer, causing surface water to seep and decreasing surface runoff. Precipitation in the Kuye River Basin is concentrated in the form of rainstorms during

Table 6 Area of vegetation restoration measures in the Kuye River basin 1960–2013 (km²)

	Afforestation area	Grassed area	Closed area
1960–1969	26.6	22.3	0
1970–1979	97.3	51.5	0
1980–1989	415	109.9	40
1990–1996	1004.3	191.6	117.2
1997	1189.5	286	117.2
1998	1245.8	295.6	117.2
1999	1311.7	305.4	117.2
2000	1400.9	314.1	119.4
2001	1497.5	331.8	132.7
2002	1614.2	367	257.6
2003	1728.4	391.6	313.2
2004	1806.3	404.8	372.2
2005	1880.8	421.5	404.6
2006	1938.3	418.5	424.8
2007	2002.6	421.9	442.1
2008	2067.5	460.1	462.2
2009	2132.3	498.3	482.4
2010	2197.2	536.5	502.5
2011	2270.1	574.8	522.7
2012	2354.5	574.8	522.7
2013	2354.5	574.8	522.7

*Data from the Statistical Yearbook

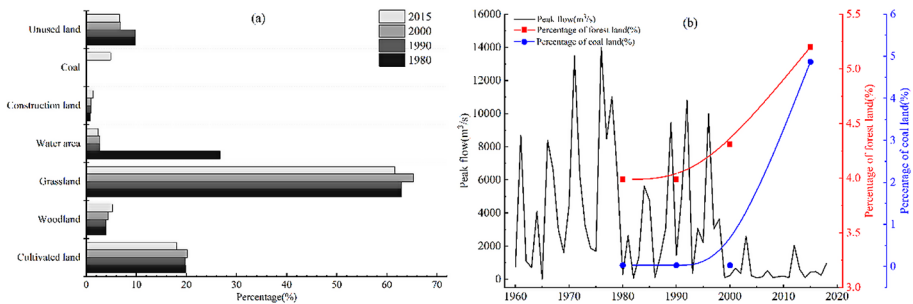


Fig. 13 (a) Proportion of land use structure in Kuye River basin; (b) Landcover change and its corresponding impact on the flooding dynamics

the flood season, and the coal mining area significantly impacts the sedimentation of the downstream river and the flood process in the basin.

4.3 Limitation

The study of the impact of human activities on flood processes is increasing, but there is still more to be done. This is just a preliminary analysis, and further questions must be investigated. There are numerous causes for the changes in the underlying surface. This work studied the effects of numerous human activities on the underlying surface. However, only vegetation change and land use change may be captured in the model, making it impos-

sible to examine the influence of human activities thoroughly and objectively. Varied human activities have different impacts on the flooding process at different times. In the subsequent study, we may assess and quantify the influence of various human actions.

5 Conclusions

Using the Kuye River basin on the Loess Plateau as an example, this research identifies the evolution of the rainstorm and flood characteristics in the basin from 1960 to 2018. It was determined that flood peak flow decreased when precipitation did not decrease. The DTVGM model is then used to quantitatively analyze the degree of reduction of the flooding process caused by the change in land use in the study area. The main findings are as follows:

- (1) From 1960 to 2018, the four rainstorm indicators of the annual maximum one h precipitation, annual maximum precipitation, the number of days with precipitation ≥ 25 mm, and the number of days with precipitation ≥ 50 mm exhibited no significant upward trend. After 2000, precipitation increased compared to the 1980 and 1990 s, during which precipitation was at its lowest level in the long-term record.
- (2) The evolution of the flood in the basin indicates that the maximum annual flood peak discharge and the frequency of large and moderate floods are decreasing. Based on a double test of the M-K mutation test and the sliding t-test, the year of flood peak flow mutation is 1998, indicating that the annual maximum flood peak flow exhibits a consistent downward trend.
- (3) The DTVGM model is used to simulate the rainstorm flood process in the base period and the change period of the Kuye River Basin, and the difference obtained from the simulation shows that the change in the land use of the basin has reduced the flood peak flow. Combined with the relationship between rainstorms and flood, it is verified that human activities lead to changes in the land use of the basin, which leads to changes in the law of flow generation and confluence in the watershed, resulting in a decrease in flood peak flow. The results provide a scientific basis for preventing and mitigating flood disasters in the basin in the future.

Acknowledgements Methodology, Lichan Li, Tong Nie; Software, Lichan Li; Validation, Yuxin Lei, Jiaying He, Wenjuan Cai; Conceptualization, Tong Nie; Formal analysis, Tong Nie; Investigation, Lichan Li; Resources, Xiaohui Jiang; Data curation, T.N.; Writing—original draft, Tong Nie; Writing—review and editing, Xiaohui Jiang; Visualization, Xiaohui Jiang; Supervision, Xiaohui Jiang; Project administration, Xiaohui Jiang; Funding acquisition, Xiaohui Jiang. All authors have read and agreed to the published version of the manuscript.

Funding This work was supported by the National Natural Science Fund (52379025, 51779209).

Declarations

Conflict of interest The authors declare no conflict of interest.

References

- Abbo H, Shavit U, Markel D, Rimmer A (2003) A numerical study on the influence of fractured regions on lake/groundwater interaction; the Lake Kinneret (Sea of Galilee). *case J Hydrol* 283:225–243. [https://doi.org/10.1016/S0022-1694\(03\)00273-7](https://doi.org/10.1016/S0022-1694(03)00273-7)
- Du R, Du R, Shang F, Shang F, Ma N, Ma N (2019) Automatic mutation feature identification from well logging curves based on sliding t test algorithm. *Cluster Comput* 22:14193–14200
- Erena SH, Worku H (2019) Dynamics of land use land cover and resulting surface runoff management for environmental flood hazard mitigation: the case of dire daw city. *Ethiopia J Hydrology: Reg Stud* 22:100598. <https://doi.org/10.1016/j.ejrh.2019.100598>
- Fu B, Wang S, Liu Y, Liu J, Liang W, Miao C (2017) Hydrogeomorphic ecosystem responses to natural and anthropogenic changes in the Loess Plateau of China. *Annu Rev Earth Pl Sc* 45:223–243. <https://doi.org/10.1146/annurev-earth-063016-020552>
- Fu S, Yang Y, Liu B, Liu H, Liu J, Liu L, Li P (2020) Peak flow rate response to vegetation and terraces under extreme rainstorms agriculture. *Ecosyst Environ* 288:106714. <https://doi.org/10.1016/j.agee.2019.106714>
- Gao J, Holden J, Kirkby M (2016) The impact of land-cover change on flood peaks in peatland basins. *Water Resour Res* 52:3477–3492. <https://doi.org/10.1002/2015WR017667>
- Gu C, Mu X, Gao P, Zhao G, Sun W (2018) Changes in run-off and sediment load in the three parts of the Yellow River basin, in response to climate change and human activities. *Hydrol Process* 33:585–601. <https://doi.org/10.1002/hyp.13345>
- Gu C, Zhu Y, Li R, Yao H, Mu X (2021) Effects of different soil and water conservation measures on hydrological extremes and flood processes in the Yanhe River, Loess Plateau. *China Nat Hazards* 109:545–566. <https://doi.org/10.1007/s11069-021-04848-w>
- Guo Q, Han Y, Yang Y, Fu G, Li J (2019) Quantifying the impacts of Climate Change, Coal Mining and Soil and Water Conservation on Streamflow in a coal mining concentrated Watershed on the Loess Plateau. *China Water-Sui* 11:1054. <https://doi.org/10.3390/w11051054>
- Gupta HV, Sorooshian S, Yapo PO (1999) Status of automatic calibration for hydrologic models: comparison with multilevel expert calibration. *J Hydrol Eng* 2(4):135–143
- Hirabayashi Y, Mahendran R, Koirala S, Konoshima L, Kanae S (2013) Global flood risk under climate change. *Nat Clim Change* 3:816–821
- Hirsch RM, Archfield SA (2015) Flood trends: not higher but more often. *Nat Clim Change* 5:198–199
- Hou J, Ye A, You J, Ma F, Duan Q (2018) An estimate of human and natural contributions to changes in water resources in the upper reaches of the Minjiang River. *Sci Total Environ* 635:901–912. <https://doi.org/10.1016/j.scitotenv.2018.04.163>
- Hu Y, Maskey S, Uhlenbrook S, Zhao H (2011a) Streamflow trends and climate linkages in the source region of the Yellow River. *China Hydrol Process* 25:3399–3411. <https://doi.org/10.1002/hyp.8069>
- Hu Y, Maskey S, Uhlenbrook S, Zhao H (2011b) Streamflow trends and climate linkages in the source region of the Yellow River. *China Hydrol Process* 25:3399–3411. <https://doi.org/10.1002/hyp.8069>
- Jiang XH, Gu XW, He HM (2010) The influence of coal mining on water resources in the Kuye River Basin. *J Nat Resour* 25(02):300–307 (in Chinese)
- Kia MB, Pirasteh S, Pradhan B, Mahmud AR, Sulaiman WNA, Moradi A (2012) An artificial neural network model for flood simulation using GIS: Johor River Basin. *Malaysia Environ Earth Sci* 67:251–264. <https://doi.org/10.1007/s12665-011-1504-z>
- Li J, Liu X, Chen F (2015) Evaluation of Nonstationarity in Annual Maximum Flood Series and the associations with large-scale climate patterns and human activities. *Water Resour Manag* 29:1653–1668. <https://doi.org/10.1007/s11269-014-0900-z>
- Li H, Shi C, Sun P, Zhang Y, Collins AL (2021) Attribution of runoff changes in the main tributaries of the middle Yellow River, China, based on the Budyko model with a time-varying. *Parameter Catena* 206:105557. <https://doi.org/10.1016/j.catena.2021.105557>
- Liang K, Liu C, Liu X, Song X (2013) Impacts of climate variability and human activity on streamflow decrease in a sediment concentrated region in the Middle Yellow River Stoch. *Env Res Risk A* 27:1741–1749. <https://doi.org/10.1007/s00477-013-0713-2>
- Liu X, Yang S, Dang S, Luo Y, Li X, Zhou X (2014a) Response of sediment yield to vegetation restoration at a large spatial scale in the Loess. *Plateau Sci China Technological Sci* 57:1482–1489. <https://doi.org/10.1007/s11431-014-5605-2>
- Liu X, Yang S, Dang S, Luo Y, Li X, Zhou X (2014b) Response of sediment yield to vegetation restoration at a large spatial scale in the Loess. *Plateau Sci China Technological Sci* 57:1482–1489. <https://doi.org/10.1007/s11431-014-5605-2>

- Liu XY, Liu CM, Yang ST, Jin SY, Gao YJ, Gao YF (2014c) Influences of shrubs-herbs-arbor vegetation coverage on therunoff based on the remote sensing data in Loess Plateau. *Acta Geogr Sin* 69(11):1595–1603 (in Chinese)
- Liu XY, Li HB, Li XY, Gao YF (2022) Analysis on the cause of sharp decrease of runoff and sediment from Kuye River in Loess Plateau. *Jouenal Hydraulic Eng* 53(03):296–305 (in Chinese)
- Luan J, Zhang Y, Tian J, Meresa H, Liu D (2020) Coal mining impacts on catchment runoff. *J Hydrol* 589:125101. <https://doi.org/10.1016/j.jhydrol.2020.125101>
- Lv C, Wang X, Ling M, Xu W, Yan D (2023) Effects of Precipitation Concentration and Human activities on City Runoff Changes. *Water Resour Manag* 37:5023–5036. <https://doi.org/10.1007/s11269-023-03593-y>
- Ma X, Shi C, Peng J, Liu W (2021) Quantitative ascription of sediment discharge changes of two highly sediment-loaded tributaries of the Yellow River in China: the importance of selecting Rainfall Index and. *Timescale Water-Sui* 13:845. <https://doi.org/10.3390/w13060845>
- Mann HB (1945) Nonparametric test against trend. *Econometrica* 13:245–259
- Mao Y, Ye A, Liu X, Ma F, Deng X, Zhou Z (2016) High-resolution simulation of the spatial pattern of water use in continental China. *Hydrol Sci J* 61:2626–2638. <https://doi.org/10.1080/02626667.2016.1153102>
- Nash JE, Sutcliffe JV (1970) River flow forecasting through conceptual models (part 1): a discussion of principles. *J Hydrol* 3(10):282–290
- Pal SC, Chowdhuri I, Das B, Chakraborty R, Roy P, Saha A, Shit M (2022) Threats of climate change and land use patterns enhance the susceptibility of future floods in India. *J Environ Manage* 305:114317. <https://doi.org/10.1016/j.jenvman.2021.114317>
- Piao S et al (2015) Detection and attribution of vegetation greening trend in China over the last 30 years. *Global Change Biol* 21:1601–1609. <https://doi.org/10.1111/gcb.12795>
- Qu S, Wang G, Shi Z, Zhou P, Xu Q, Zhu Z (2020) Temporal changes of hydraulic properties of overburden aquifer induced by longwall mining in Ningxiaota Coalfield, northwest. *China J Hydrol* 582:124525. <https://doi.org/10.1016/j.jhydrol.2019.124525>
- Ren S, Han X, Yang J, Tang S, Zhang Y, Shan T, Liu C (2022) Global rainstorm disaster risk monitoring based on Satellite Remote sensing. *J Meteorological Res* 36:15
- Sheng F, Liu S, Zhang T, Liu G, Liu Z (2022) Quantitative assessment of the impact of precipitation and vegetation variation on flooding under discrete and continuous rainstorm conditions. *Ecol Indic* 144:109477. <https://doi.org/10.1016/j.ecolind.2022.109477>
- Szwagrzyk M, Kaim D, Price B, Wypych A, Grabska E, Kozak J (2018) Impact of forecasted land use changes on flood risk in the Polish. *Carpathians Nat Hazards* 94:227–240. <https://doi.org/10.1007/s11069-018-3384-y>
- Wang H, Yang Z, Saito Y, Liu JP, Sun X, Wang Y (2007a) Stepwise decreases of the Huanghe (Yellow River) sediment load (1950–2005): impacts of climate change and human activities. *Global Planet Change* 57:331–354. <https://doi.org/10.1016/j.gloplacha.2007.01.003>
- Wang H, Yang Z, Saito Y, Liu JP, Sun X, Wang Y (2007b) Stepwise decreases of the Huanghe (Yellow River) sediment load (1950–2005): impacts of climate change and human activities. *Global Planet Change* 57:331–354. <https://doi.org/10.1016/j.gloplacha.2007.01.003>
- Wang H, Bi N, Saito Y, Wang Y, Sun X, Zhang J, Yang Z (2010) Recent changes in sediment delivery by the Huanghe (Yellow River) to the sea: causes and environmental implications in its estuary. *J Hydrol* 391:302–313. <https://doi.org/10.1016/j.jhydrol.2010.07.030>
- Wang GQ et al (2013) Simulating the impact of Climate Change on Runoff in a typical river catchment of the Loess Plateau. *China J Hydrometeorol* 14:1553–1561. <https://doi.org/10.1175/JHM-D-12-081.1>
- Wang Q, Xu Y, Wang J, Lin Z, Dai X, Hu Z (2019) Assessing sub-daily rainstorm variability and its effects on flood processes in the Yangtze River Delta region. *Hydrol Sci J* 64:1972–1981. <https://doi.org/10.1080/02626667.2019.1645332>
- Wang Q, Xu Y, Cai X, Tang J, Yang L (2021) Role of underlying surface, rainstorm and antecedent wetness condition on flood responses in small and medium sized watersheds in the Yangtze River Delta region. *China Catena* 206:105489. <https://doi.org/10.1016/j.catena.2021.105489>
- Xia J, Wang GS, Tan G, Ye AZ, Huang GZ (2004) Hydrological nonlinear systems and distributed time-varying gain models. *Chin Sci (Series D: Earth Sci)* (11), 1062–1071. (in Chinese)
- Xia J, Wang Q, Zhang X, Wang R, She D (2018) Assessing the influence of climate change and inter-basin water diversion on Haihe River basin, eastern China: a coupled model approach. *Hydrogeol J* 26:1455–1473. <https://doi.org/10.1007/s10040-018-1773-7>
- Xia R, Sun H, Chen Y, Wang Q, Chen X, Hu Q, Wang J (2023) Ecological Flow Response Analysis to a typical strong hydrological Alteration River in China *Int. J Env Res Pub He* 20. <https://doi.org/10.3390/ijerph20032609>
- Yang P et al (2022) Effects of climate change on major elements of the hydrological cycle in Aksu River basin. *Northwest China Int J Climatol*

- Yang Y, Zhang W, Liu Z, Liu D, Huang Q, Xia J (2023) Coupling a distributed time variant Gain Model into a Storm Water Management Model to Simulate runoffs in a sponge. *City Sustainability-Basel* 15:3804. <https://doi.org/10.3390/su15043804>
- Yao H, Shi C, Shao W, Bai J, Yang H (2016) Changes and influencing factors of the sediment load in the Xiliugou basin of the upper Yellow River. *China Catena* 142:1–10. <https://doi.org/10.1016/j.catena.2016.02.007>
- Yu J, Zou L, Xia J, Dou M, Liu H, Zuo L (2023) Future changes in hydrological drought across the Yangtze River Basin: identification, spatial–temporal characteristics, and concurrent probability. *J Hydrol* 625:130057. <https://doi.org/10.1016/j.jhydrol.2023.130057>
- Zare M, Samani AAN, Mohammady M (2016) The impact of land use change on runoff generation in an urbanizing watershed in the north of Iran. *Environ Earth Sci* 75. <https://doi.org/10.1007/s12665-016-6058-7>
- Zhang Q, Gu X, Singh VP, Kong D, Chen X (2015) Spatiotemporal behavior of floods and droughts and their impacts on agriculture in China. *Global Planet Change* 131:63–72. <https://doi.org/10.1016/j.gloplacha.2015.05.007>
- Zhang J, Gao G, Fu B, Gupta HV (2020) Investigation of the relationship between precipitation extremes and sediment discharge production under extensive land cover change in the Chinese Loess Plateau. *Geomorphology* 361:107176. <https://doi.org/10.1016/j.geomorph.2020.107176>
- Zhao G, Mu X, Wen Z, Wang F, Gao P (2013) SOIL EROSION, CONSERVATION, AND ECO-ENVIRONMENT CHANGES IN THE LOESS PLATEAU OF CHINA. *Land Degrad Dev* 24:499–510. <https://doi.org/10.1002/ldr.2246>
- Zhao G et al (2016) Evidence and causes of spatiotemporal changes in runoff and sediment yield on the Chinese Loess Plateau. *Land Degrad Dev* 28:579–590. <https://doi.org/10.1002/ldr.2534>
- Zhu F, Zhong PA, Sun Y, Yeh WWG (2017) Real-time optimal Flood control decision making and risk propagation under multiple uncertainties. *Water Resour Res* 53:10635–10654. <https://doi.org/10.1002/2017WR021480>
- Zuo D, Wu C, Zheng Y, Chen X, Wang L (2023) Climate change and human activity impacts on future flood risk in the Pearl River Delta based on the MaxEnt. *Model Front Earth Sc-Switz* 10. <https://doi.org/10.3389/feart.2022.1053829>

Publisher's Note Springer Nature remains neutral with regard to jurisdictional claims in published maps and institutional affiliations.

Springer Nature or its licensor (e.g. a society or other partner) holds exclusive rights to this article under a publishing agreement with the author(s) or other rightsholder(s); author self-archiving of the accepted manuscript version of this article is solely governed by the terms of such publishing agreement and applicable law.